



**University of
Zurich**^{UZH}

**Zurich Open Repository and
Archive**

University of Zurich
University Library
Strickhofstrasse 39
CH-8057 Zurich
www.zora.uzh.ch

Year: 2023

Small-scale spatial beta diversity of bacteria in the mixed upper layer of a lake

Pernthaler, Jakob ; Krempaska, Natalia ; Le Moigne, Alizée

DOI: <https://doi.org/10.1111/1462-2920.16399>

Posted at the Zurich Open Repository and Archive, University of Zurich

ZORA URL: <https://doi.org/10.5167/uzh-233960>

Journal Article

Published Version



The following work is licensed under a Creative Commons: Attribution 4.0 International (CC BY 4.0) License.

Originally published at:

Pernthaler, Jakob; Krempaska, Natalia; Le Moigne, Alizée (2023). Small-scale spatial beta diversity of bacteria in the mixed upper layer of a lake. *Environmental Microbiology*, 25(10):1847-1859.

DOI: <https://doi.org/10.1111/1462-2920.16399>

RESEARCH ARTICLE

Small-scale spatial beta diversity of bacteria in the mixed upper layer of a lake

Jakob Pernthaler  | Natalia Krempaska | Alizée le Moigne

Limnological Station, Department of Plant and Microbial Biology, University of Zurich, Zurich, Switzerland

Correspondence

Jakob Pernthaler, Limnological Station, Department of Plant and Microbial Biology, University of Zurich, 8802 Zurich, Switzerland. Email: pernthaler@limnol.uzh.ch

Funding information

Schweizerischer Nationalfonds zur Förderung der Wissenschaftlichen Forschung, Grant/Award Number: 31003A_182336; Universität Zürich, URPP "Biodiversity and Global Change"

Abstract

Bacterial community composition among individual, experimentally generated 'lake snow' particles may be highly variable. Since such aggregates are seasonally abundant in the mixed upper layer of lakes, we hypothesized that particle-attached (PA) bacteria disproportionately contribute to the small-scale spatial beta diversity of pelagic communities. Community composition was analysed in sets of small (10 mL) samples collected from a pre-alpine lake in May, July and October 2018. Bacteria were classified as free-living (FL) or PA depending on their presence in large, 5- μm pre-filtered reference samples. FL exhibited clear seasonal differences in community composition and assembly. They were spatially uniform in May and July, and only a few FL taxa exhibited significant spatial variability. Spatial heterogeneity of FL in October was caused by high alpha and beta diversity of rare taxa, many with a presumably 'tychoplanktic' (alternating attached and free-living) lifestyle. The spatial beta diversity of PA was always high, and only about 10% of their seasonal richness was present in any single sample. Thus, most compositional variability of pelagic bacteria at spatial scales of cm to m either directly or indirectly originated from PA. On a functional level, this genotypic heterogeneity might affect the spatial distribution of rare metabolic traits.

INTRODUCTION

Physical, chemical and biological factors act on pelagic microbial communities in lakes at various spatial scales: Large-scale structuring of the water body by thermal stratification and wind-driven current systems (Imboden & Wuest, 1995) is reflected in vertical and horizontal distribution patterns of planktonic bacteria (Hu et al., 2020; Okazaki et al., 2017; Salcher et al., 2011). Distances of dozens of metres to kilometres lead to a decline in similarity among local pelagic microbial communities mainly as a consequence of habitat gradients (Jones et al., 2012; Lear et al., 2014), and in agreement with predictions of the macroecological 'distance decay' concept (Morlon et al., 2008; Soininen et al., 2007). At the smallest spatial scales, there are millimetre to sub-millimetre

heterogeneities of dissolved organic substrate concentrations, for example, the immediate surroundings of single phytoplankton cells (Seymour et al., 2017), or the solute plumes of sinking detrital particles (Kjørboe & Jackson, 2001).

Less information is available about heterogeneity within pelagic bacterial assemblages at distances ranging from centimetres to metres. At such scales, the epilimnetic zone of lakes is structured by turbulent vertical mixing and advection (Wuest & Lorke, 2003), resulting in transient local patterns of actively mixing water patches and a hierarchy of increasingly smaller and short-lived turbulent eddies. The concentrations of labile substrates (dissolved free amino acids, DFAAs) may differ by orders of magnitude within centimetre distances as a consequence of, both, physical and biological processes (Krempaska et al., 2021). Arguably,

This is an open access article under the terms of the [Creative Commons Attribution](https://creativecommons.org/licenses/by/4.0/) License, which permits use, distribution and reproduction in any medium, provided the original work is properly cited.

© 2023 The Authors. *Environmental Microbiology* published by Applied Microbiology International and John Wiley & Sons Ltd.

these scales are particularly relevant for the interactions of bacteria with a predominantly free-living lifestyle with others that are mainly particle-associated (subsequently referred to as 'FL and PA sub-communities'): Depending on the season, the concentration of 'lake snow' in a deep pre-alpine lake may range from a few to $>50\text{ L}^{-1}$ of surface water (Grossart & Simon, 1998). By comparison, the abundance of 'marine snow' particles may vary between <1 and $>10\text{ L}^{-1}$ in the Northeast Atlantic (Lampitt et al., 1993), and reach $>25\text{ L}^{-1}$ in the pycnocline of the Baltic Sea (Möller et al., 2012). 'Lake snow' particles are mainly colonized by taxa that are rare in the water column (Allgaier & Grossart, 2006; Tang et al., 2010). Nevertheless, the two sub-communities may at times substantially overlap (Bizic-Ionescu et al., 2015), indicating that a proportion of PA bacteria are likely 'tychoplanktic': they temporarily switch to a free-living, motile, lifestyle to chemotactically track and exploit local substrate gradients (Raina et al., 2022).

Thus, the assembly of pelagic bacterial (meta)communities at centimetre to metre scales should be an interplay of homogenizing processes, namely turbulent mixing (Vincent & Meneguzzi, 1991), and of processes that generate variabilities, such as priority effects, deterministic selection, or dispersal limitation (Bizic-Ionescu et al., 2018; Datta et al., 2016; Lear et al., 2014). Conceptionally, most heterogeneity within pelagic bacterial communities at this scale should either originate from PA (Bizic-Ionescu et al., 2018) or from tychoplanktic bacteria with small FL subpopulations. By contrast, the numerically abundant FL taxa should largely be homogenized by physical mixing. However, some predominantly free-living bacteria might still exhibit variability at this scale, for example, due to non-synchronized local growth in a variable substrate field (Horňák et al., 2016; Krempaska et al., 2021) or spatially uneven distribution of viral lysis (Dann et al., 2016; Seymour et al., 2006). It is conceivable that such compositional heterogeneity would also have functional consequences, for example, with respect to the spatial distribution of rare metabolic traits that are required to degrade recalcitrant chemical compounds (Seller et al., 2020).

We analysed the variability of the pelagic FL and PA bacterial sub-communities in small volumes of water (10 mL) collected at distances of centimetres to metres during three campaigns from the mixed upper layer of Lake Zurich. Larger samples (600 mL) from the same depth and pre-filtered through 5- μm pore-size filters served to operationally distinguish between FL and PA (Allgaier & Grossart, 2006; Hu et al., 2020; Rösel et al., 2012). We tested the hypothesis that the spatial beta diversity of PA in bacterial communities from the small samples was higher than that of FL. In addition, we explored if any FL populations exhibited significant spatial variability or were related to the spatial patterns

of a class of labile substrates (DFAA, determined in a previous study) (Krempaska et al., 2021).

EXPERIMENTAL PROCEDURES

Sampling

Lake Zurich ($47^{\circ}19'21''\text{ N}$, $8^{\circ}33'42''\text{ E}$) is a large, deep, mesotrophic pre-alpine lake (406 m asl, area 65.06 km^2 , max. depth 136 m, mean depth 51.7 m, residence time 440 days, $\text{N}47^{\circ}17.147'$, $\text{E}8^{\circ}35.460'$, Switzerland) (Bossard et al., 2001). The dominant primary producer in the lake is the toxic filamentous cyanobacterium *Planktothrix rubescens* (Posch et al., 2012).

Water samples were taken on May 9th, July 20th and October 5th 2018 at 5 m depth near the deepest point. A custom-built sampling device was used to assess the small-scale spatial variability of the bacterial metacommunity at two spatial scales (cm to m). Its design, use, and storage between campaigns are described in detail in Krempaska et al. (2021), where it served to assess the variability of DFAA at different seasons over 3 years. Briefly, 10 adjacent water samples were simultaneously collected from a depth of 5 m in 10 mL syringes spaced at distances of 2 cm (subsequently referred to as 'syringe samples'). Freshly collected samples were transferred into sterile 15 mL plastic tubes. The sampling procedure was repeated 10 times to collect replicate sample sets, at approximate intervals of 5 min, which was the time required for sample handling and reequipping the device with the syringes. One additional water sample (subsequently referred to as 'reference sample') was obtained from the same depth with a 5 L-Friedringer sampler (Uwitec, Mondsee, Austria) and collected in a 2 L-glass bottle (Schott, Germany). Samples were transported to the laboratory in the dark at in situ temperature within an hour and split into subsamples for DFAA analysis (reported in (Krempaska et al., 2021)), flow cytometry, and the amplification of bacterial 16S *rRNA* genes.

Vertical chlorophyll *a* (Chl *a*) concentration profiles were determined with a TS-16-12 fluoroprobe (bbe Mol-daenke, Kronshagen, Germany). This multi-wavelength probe was calibrated to distinguish between major groups of phytoplankton based on their pigment fluorescence spectra (Beutler et al., 2002). Temperature profiles were measured with an YSI multi-parameter probe (6600 YSI, Yellow Springs, OH, USA).

Bacterial abundances of cells with high and low nucleic acid content

A 1 mL subsample from each syringe sample and ten 1-mL-subsamples from the 2 L reference sample were

fixed with 37% formaldehyde (final concentration 2%) for flow cytometric analysis. Portions of 180 μ L from these samples were then transferred onto 96-well microtitre plates, for 30 min, stained with SYBR green (Sigma- Aldrich, Saint Louis, MO, USA) in DMSO for (final concentration, 5%), and analysed on a CytoFLEX flow cytometer (Beckman Coulter, Brea, CA, USA) within 24 h after collection.

The resulting scatter plots of SYBR fluorescence intensity versus side scatter were analysed with the software CytExpert (Beckman Coulter) to determine the total number of cells and the respective proportions of cells with high and low nucleic acid content (HNA, LNA) (Salcher et al., 2007). Since initial tests indicated that there were systematic differences in the proportions of HNA and LNA bacteria between plates, but not within a single plate (data not shown), only 8 of the 10 sets of syringe samples (80 samples) from May, July and October 2018, respectively, were analysed. To further assess the technical variability of flow cytometric measurements, one additional 96-well plate of subsamples from the reference sample per season was stained and measured as described above.

Seasonal differences in the abundances of all bacteria as well as of HNA and LNA cells were assessed by a two-way analysis of variance (ANOVA). Data were log-transformed to approximate normality. The spatial variability of HNA and LNA cells was examined by calculating the coefficients of variation (CV) for each set of 10 adjacent syringe samples and the set of 10 subsamples from the well-mixed reference sample. Differences in the CVs of HNA and LNA bacteria between seasons were tested for significance by the Wilcoxon rank sum test. All statistical tests were performed in R (version 3.5.2, package *stats*).

DNA extraction, 16S rRNA gene amplification and sequence analysis

Portions of 1 mL were collected from the syringe samples in sterile tubes (Eppendorf, PCR clean) and stored at -24°C until further processing. Samples with the five lowest and five highest DFAA concentrations per sampling set were chosen for 16S rRNA gene sequencing. Additional pairs or triplets of adjacent samples with very high versus very low concentrations were also included for sequencing. Altogether, 19 syringes were selected from the May and October campaigns, and 24 from July (see Figure S3 for details of which samples were selected). In addition, two sets of 5 technical replicates originating from two different syringes were produced for each season.

A custom PCR protocol was developed to amplify 16S rRNA genes from small sample volumes. For this, portions of 100 μ L were taken from the 1 mL subsamples and centrifuged for 1 h at 12°C at maximum speed

(approximately 20,000g). The supernatant was discarded and the sample pellet was lysed using alkaline lysis from the Repli-g Single Cell Kit (Qiagen, Germany) for 10 min at 65°C . DNA extraction and purification were performed with Sera-Mag speed beads (GE Healthcare) in a custom-made buffer (protocol available online: https://s3-us-west-2.amazonaws.com/oww-files-public/f/f8/SPRI_buffers_v2_2.pdf) and following the procedure outlined in the Agencourt AMPure XP PCR Purification kit (Beckman Coulter). The following modifications were made for DNA extraction: the same volume of magnetic beads was added as the sample volume; samples were incubated with magnetic beads for 10 min at room temperature; tubes were placed on a magnetic rack for 3–5 min to separate beads from the solution. After discarding the clear solution, 1 mL of freshly prepared 70% ethanol was added with the tubes still on the magnetic rack. This washing step was repeated after 30 s with 200 μ L of 70% ethanol. Elution time was extended to 1 h at 37°C . PCR of partial 16S rRNA genes was performed with a KAPA HiFi HotStart PCR kit (Kapa Biosystems, Roche) for 30 cycles using the primer pair 799f–1115mod r (Chelius & Triplett, 2001; Silva et al., 2018). The reproducibility of the protocol was evaluated by comparing the similarity of replicate communities generated from single syringes (see above).

For analysis of the reference samples collected with the 5 L Friedinger sampler, triplicate portions of 600 mL were first pre-filtered through 5 μ m (Whatman Nucleopore) and then filtered on polyethersulfone (PES) filters (Millipore Express, pore size 0.22 μ m). DNA extraction was performed using the DNeasy PowerBiofilm Kit (Qiagen, Germany) following the manufacturer's protocol, doubling the amount of reagent volume and with an extension of the inhibitor-removal step to 1 h. Extracted DNA from reference samples was purified as described above using the Sera-Mag speed beads and following the procedure outlined in the Agencourt AMPure XP PCR Purification kit (Beckman Coulter). PCR amplification of partial 16S rRNA genes from these extracts (primers 799f –1115mod r) as well as the sequencing of these amplicons (Illumina MiSeq) was performed by LGC Genomics (Germany). The processing of raw sequencing data, the calling of operational taxonomic units (OTUs), and their taxonomic assignment was carried out with an in-house analysis pipeline as described before (Silva et al., 2018). Briefly, the pipeline included the joining of paired reads and the trimming of amplicons to a length of 300 bases, dereplication, quality control (an average error rate of 0.5 per sequence), chimera check and the definition of operational taxonomic units (OTUs) by a clustering algorithm comparable to UNOISE2 (Edgar, 2016). Taxonomic assignment was performed by a BLAST search of the representative sequences of individual OTUs against the SILVA database (version 138) (Quast et al., 2013).

Operational definition of FL and PA

It was not feasible to physically separate PA from FL bacteria in the 10 mL syringe samples. Therefore, we adopted an *in silico* strategy to assign OTUs to either sub-community based on OTUs present or absent in the pre-filtered reference samples. The complete sequence dataset was divided into subsets, as schematically outlined in Figure S1: all OTUs in syringe samples that were also present in any of the 5 μm pre-filtered reference samples from the same date were operationally classified as members of FL, assuming that the much larger water volume of the combined reference samples (3×600 mL) would provide a comprehensive collection of FL bacteria. The remaining OTUs in syringe samples were assigned to PA. A third data set comprised all OTUs of FL in the technical replicates from single syringes (subsequently termed ‘Replicates’). FL and replicate data sets were then separately normalized to 10,000 reads per sample using the ‘rarefy_even_depth’ function of the R package *phyloseq*. Four of the altogether 92 samples were excluded from further analyses because the total read numbers in these samples were below this threshold.

Bacterial diversity, community composition and assembly processes

To assess the extent of spatial heterogeneity, we compared the ‘within-sample’ and ‘total’ (all samples combined) alpha diversity (OTU richness) of FL and PA in 100 μL samples from the 10 mL syringes, as well as in the 600 mL reference samples collected with a 5 L sampler.

The seasonal differences in community composition among reference samples, FL and PA were analysed by principal coordinates analysis (PCoA, Bray–Curtis dissimilarity) with the R package *ape* (Paradis & Schliep, 2019). A PERMANOVA was then performed to examine the significance of the seasonal differences (function *adonis* in R package *vegan*) (Oksanen et al., 2018). Pairwise comparisons were subsequently performed using the function *pairwise.perm.manova* from R package *RVAideMemoire* (Hervé, 2020), correcting for multiple testing by the false discovery rate (fdr) method (Benjamini & Hochberg, 1995). A similarity percentage analysis (SIMPER) was performed to identify OTUs that most significantly contributed to the distinction between seasons (R package *vegan*). The dominant seasonal assembly process of the bacterial communities in the syringes was assessed with the normalized stochasticity ratio (NST) (Ning et al., 2019).

We tested if FL in replicates from single syringes were more similar to each other than sub-communities originating from different syringes. Pairwise modified Raup–Crick indices (RC) were separately calculated for

FL of the syringe and replicate samples with the R package *NST* (Ning et al., 2019). This approach was also used to test if pairs of sub-communities that originated from sets of 10 simultaneously collected syringe samples (e.g., samples A1 vs. A5) were more similar to each other than pairs that originated from different sets (e.g., samples A1 vs. J1). Differences between the respective proportions of significantly similar pairs (RC values < -0.95) were then tested for significance with a two-proportional z-test.

Spatial variability of abundant OTUs from FL

We tested if abundant OTUs from FL had significantly higher variability between individual syringes than among replicates from single syringes. ‘Abundant OTUs’ were operationally defined by average read numbers >10 in the syringes and each of the 2 sets of 5 replicates. Analyses were performed separately for each season. First, we calculated the absolute differences between the read numbers of each OTU in individual replicates and their respective means in all replicates. These differences were then normalized by dividing them by their means and fitted to various theoretical distributions, using Kolmogorov–Smirnov and Anderson–Darling tests to assess goodness of fit (EasyFit 5.5, MathWave Technologies). The distribution that scored highest in both tests (subsequently termed ‘test distribution’) was selected to assess the significance of OTU variability in the syringe samples. For each OTU, we first identified the syringe sample with the highest deviation from the mean and determined its *p*-value from the probability density function of the test distribution. These *p*-values were then corrected for multiple testing by the Benjamini–Hochberg method.

Relationship between OTUs from FL and DFAA concentrations

We investigated if the read numbers of abundant OTUs in the syringe samples were significantly correlated with DFAA concentrations. To circumvent a type I error of multiple testing, a null model was generated separately for each season by calculating Spearman rank correlations between the read numbers of individual OTUs and randomized DFAA concentrations (1000 randomizations, i.e., $>200,000$ correlation coefficients from randomized data per season). Only those correlations between OTUs and the original DFAA data were deemed significant that had correlation coefficients $<0.5\%$ or $>99.5\%$ than the correlation coefficients obtained from the randomized dataset. In addition, only those OTUs were considered that were present in at least half of the samples per sampling campaign.

RESULTS

Environmental conditions

At the beginning of May, there were distinct phytoplankton maxima at 5 m and 12.5 m depth, with Chl *a* concentrations of 8 and 10.7 $\mu\text{g L}^{-1}$, respectively (Figure S2). Diatoms (*Fragilaria*) and Chrysophyceae (*Uroglena*, *Dinobryon*) were mainly observed at 5 m depth, and *Planktothrix rubescens* was the dominating primary producer at 12 m depth. In July, with the setting of thermal stratification, Chl *a* concentrations at 5 m were low, indicative of a clear-water phase, whereas *P. rubescens* formed a dense layer in the metalimnion (Figure S2). In October, at the beginning of surface mixis, epilimnetic Chl *a* concentrations were almost exclusively due to *P. rubescens* being entrained into the epilimnion (Figure S2).

Total DFAA concentrations from the three campaigns are given in (Krempaska et al., 2021), and are cited here for reference. DFAA concentrations in 100 syringe samples varied by 1 to >2 orders of magnitude around the median value, with rare ‘hotspots’ of extremely high concentrations (Figure S3). The median DFAA concentration in May was 22 nM, with individual syringe samples ranging between 2.5 and 436 nM. In July, the median DFAA concentration was virtually identical to May (21.5 nM), and the overall range of variability was only about half as large (6–244 nM). In October, the median DFAA concentration was about five times higher than at the other dates (110 nM, range 31–1759 nM).

Abundances of HNA and LNA bacteria

Bacterial abundances as well as HNA and LNA in syringe samples differed between seasons (two-way ANOVA, $F = 26,775$, $p < 0.001$; $F = 2808$, $p < 0.001$), and there was a seasonal effect on the difference between HNA and LNA ($F = 64$, $p < 0.001$) (Figure 1A). HNA and LNA were surprisingly uniform across 80 syringe samples (8 sets of 10 adjacent samples, Figure S3); their overall coefficient of variation (CV) was <10% in all three seasons. Still, the CVs of HNA in 10 adjacent syringe samples in May were higher than those of LNA (Wilcoxon test, $p < 0.01$) (Figure 1B). Moreover, the CVs of HNA in these samples were all higher than in 10 technical replicates from a single haul with a 5 L sampler (‘HNF Ref’, Figure 1B). In July and October, the small-scale variability of HNA and LNA either did not significantly differ from each other or fell within the background variability of a single, repeatedly measured sample (Figure 1B, dashed lines).

Within-sample and total microbial alpha diversity

The total dataset comprised 3.7×10^6 reads prior to normalizations. The normalized FL dataset consisted of 427 OTUs (677/973 reads). The FL ‘core’ community, defined as those OTUs that were present in all syringe and reference samples from all three seasons, consisted of 30 OTUs that on average represented 78% of all reads. The PA data set included 777 OTUs (65/921 reads).

The total richness of OTUs from FL (i.e., the sum of OTUs in all 3 reference samples) was 211, 277 and 337 in May, July and October, respectively. The cumulative OTU richness of all syringe samples was 87% of the total richness of the respective reference samples in May, 94% in July and 96% in October. The median within-sample alpha diversity in individual syringe samples was between 50% and 60% of total alpha diversity (Figure 2). If all seasons were pooled, there was no significant difference between the relative alpha diversity in single syringe samples ($50\% \pm 5\%$) or single reference samples ($50\% \pm 6\%$) (Mann–Whitney U test, $p = 0.64$). The total OTU richness of bacteria in PA was 301, 222 OTUs and 512 OTUs in May, July and October, respectively. The within-sample alpha diversity of bacteria in PA was <10% of the total alpha diversity in May and July, and slightly but not significantly higher in October.

Seasonal differences in bacterial community composition and assembly processes

Overall Bray–Curtis dissimilarity between May and July was 0.57, 0.46 between May and October, and 0.44 between July and October. The differences between seasons were most strongly defined by the read proportions of *Ca. Nanopelagicus abundans* MMS-IIB-91 (May–July, July–October) and of *Ca. Planktophila lacus* MMS-IIB-106 (May–October, SIMPER, analysis) (data not shown). Bacteria from FL were mainly responsible for the dissimilarity between seasons, as visualized by PCoA (Figure 3A). A quasi-identical separation of communities between seasons was obtained if only 30 OTUs of the ‘core’ community were considered (Figure 3B). The differences between seasons among FL and ‘core’ FL were highly significant, as assessed by PERMANOVA ($p < 0.001$; FL: pseudo- $F = 316.9$; FL ‘core’: pseudo- $F = 405.1$; FL: $R^2 = 0.92$; FL ‘core’: $R^2 = 0.94$). By contrast, there was only a very poor separation of PA between seasons, and the main PCoA axes only explained a small proportion of overall variability (Figure 3c). Nevertheless, PERMANOVA

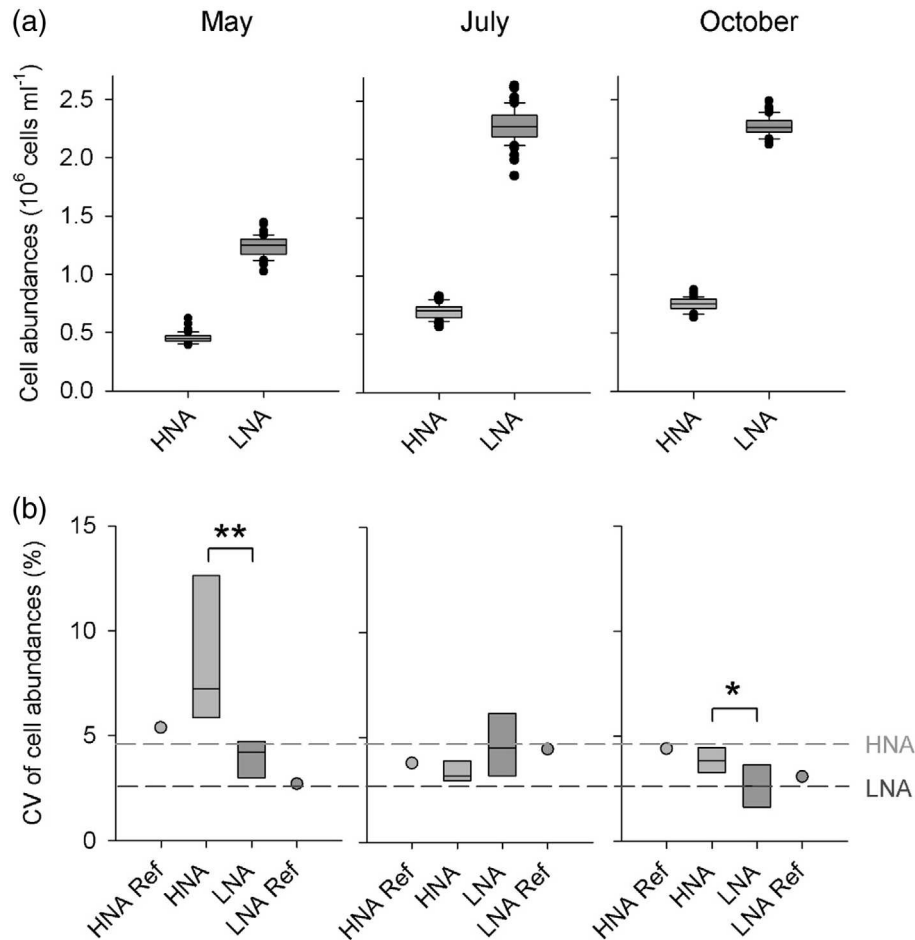


FIGURE 1 (A) Ranges of abundances of cells with a high (HNA) or low nucleic acid (LNA) content in sets of 80 syringe samples collected on May 9th, July 20th and October 5th, 2018. (B) Coefficient of variation (CV) of HNA and LNA bacteria in 8 sets of 10 syringe samples simultaneously collected at 2 cm distances (box plots) and in 10 reference samples collected with a 5 L sampler (symbols). The dashed lines indicate the average level of 'background' variability (CVs) of HNA and LNA bacteria in technical replicates from each season (i.e., 8 sets of 10 measurements of single samples). Asterisks: significant difference between CVs of HNA and LNA bacteria (** $p < 0.01$, * $p < 0.05$).

analysis also found significant differences between seasons among PA ($p < 0.001$), albeit with a small effect size (pseudo- $F = 2.7$) and a low proportion of explained variability ($R^2 = 0.09$). In May and October, we also observed a separation of communities that were either amplified from 100 μL syringe or 600 mL reference samples (Figure 3A). This could largely be ascribed to differences between the read proportions of the 30 OTUs from the 'core' community (Figure 3B).

Both, the total communities and bacteria in FL from May and July showed clear indications of being seasonally determined, with normalized stochasticity ratios (NST) $< 35\%$ (Table 1). By contrast, significantly higher NST values indicated that there was no distinct October community, but that the conditions during this period must have been equally favourable for some abundant genotypes (e.g., related to different genera of *Actinobacteria*) that were either successful in spring or in summer. The seasonal differences in assembly processes largely reflected the pattern defined by the

30 'core' OTUs, highlighting the robustness of the observed pattern (Table 1).

Beta diversity of FL between and within individual syringes

To assess spatial beta diversity of FL between syringe samples we determined the proportions of highly similar pairs of FL (i.e., $\text{RC} < -0.95$) from different syringes and technical replicates of single syringes, using the alpha-diversity independent modified Raup-Crick index (Chase et al., 2011; Ning et al., 2019). In May and July, there was no significant difference between these proportions (Figure 4). By contrast, in October, the proportion of highly similar FL pairs from different syringes was significantly smaller than from technical replicates (49% vs. 95%, z -test, $p < 0.001$). This higher difference of FL subcommunities between than within syringes could be explained by two factors: On the one

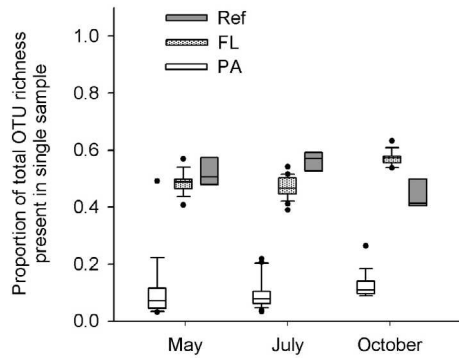


FIGURE 2 Proportion of the total seasonal richness of operational taxonomic units (OTU) from the free-living (FL) or PA sub-communities that was found in single syringe samples, and single, reference samples (FL only). Reference (ref): OTUs in 3 replicate of reference samples (600 mL volume, 5- μ m pre-filtered); FL, PA: OTUs in 100 μ L subsamples from 19 (May), 24 (July), and 19 (October) syringes that either were (FL) or were not (PA) present in ref.

hand, there was a substantially higher number of rare FL OTUs per syringe sample (defined as FL OTUs with an average of ≤ 10 reads across all syringe samples) in October (95 ± 5 , mean ± 1 SD) than in May (47 ± 6) or July (56 ± 7). On the other hand, the beta diversity of these rare OTUs (i.e., their compositional difference between syringes) was also significantly higher in October ($RC = -0.1 \pm 0.48$, mean ± 1 SD) than either in May ($RC = -0.92 \pm 0.13$) or July ($RC = -0.92 \pm 0.2$) (Kruskal–Wallis test, $N = 137$, $p < 0.001$).

OTUs from FL with significant spatial variability

Significant spatial heterogeneity could only be shown for 5 of 156 tested OTUs, all of them in samples from May (Figure 5). Three of those, affiliated with *Limnohabitans* sp. Jirll-27, *Algoriphagus aquatilis* strain A8-7, an uncultured *Sphingobacterium* previously detected in Lake Zurich (ZS-4-150), were abundant members of the OTU ‘core’ community that together formed between 4% and >13% of total reads in the May samples (Figure 5). Some of these OTUs had similar spatial distribution patterns, that is, there were highly significant positive correlations between *A. aquatilis* and *Sphingorhabdus rigui* (Pearson’s $r = 0.85$, $p < 0.01$), or *A. aquatilis* and the uncultured *Sphingobacterium* ZS-4-150 ($r = 0.84$, $p < 0.01$).

OTUs from FL associated with DFAA concentrations

No OTU in syringe samples was significantly correlated with total DFAA concentrations in May, and only one negative correlation was deemed significant in October

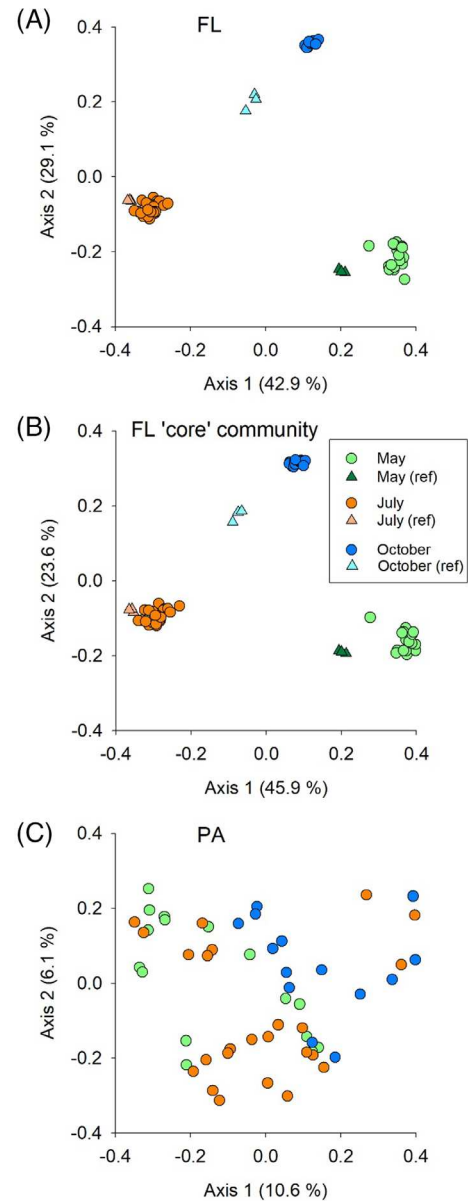


FIGURE 3 Principal coordinates analysis of communities in 100 μ L subsamples from syringes and in 600 mL subsamples of 5 μ m pre-filtered reference (ref) samples in May (M), July (J), and October (O) (A) Free-living (FL): 427 OTUs that were found in both, syringe and reference samples (B) FL core community of 30 OTUs present in all syringe and reference samples from all sampling dates, and (C) PA: 777 OTUs in syringe samples that were absent in reference samples.

(*Ignavibacteria*, HQ856347, 99.7% sequence identity). In July, 4 OTUs in FL that together formed 4% of total reads were significantly and positively associated with DFAA concentrations (with a Spearman correlation coefficient >99.5% than coefficients in the randomized data set) (Figure 6A). These OTUs were related to *Terimonas aquatica* (NR_116608, 96% sequence identity), to an uncultured bacterium from Lake Zurich affiliated with *Cryomorpaceae* (EU801285, 100% sequence identity), to an *acl* genotype from Lake Zurich

TABLE 1 Normalized stochasticity ratios (NST) of microbial communities collected in individual syringes (May, $n = 19$, July: $n = 24$, October: $n = 19$).

	Total community	FL	FL core community
May	34.2%	34.8%	33.8%
July	32.9%	32.5%	46.2%
October	62.4%	61.8%	66.9%

Note: Free-living (FL) only includes operational taxonomic units (OTUs) that were also present in large (600 mL), 5 μm pre-filtered reference samples. The 'FL core community' comprised 30 OTUs that were present in every single syringe and reference sample at all three seasons. Significance was estimated by bootstrapping (** $p < 0.001$; ** $p < 0.01$; * $p < 0.05$).

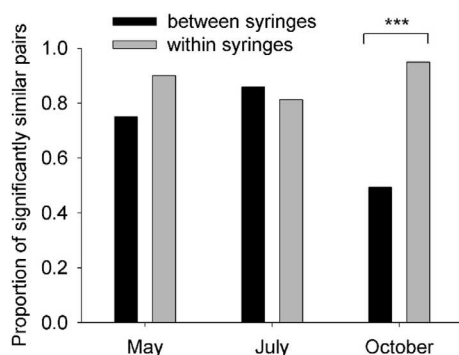


FIGURE 4 Proportions of pairs of free-living (FL) communities that were significantly more similar than expected by chance (i.e., modified Raup–Crick index < -0.95). Pairwise comparisons were performed separately for communities from different 10 mL syringes and communities from technical replicates drawn from single syringes. Significant differences in these proportions between and within syringes were only observed in October ($p < 0.001$).

(FN668306, 100% sequence identity), and a recently isolated strain from the freshwater *acIV* subcluster A of *Actinobacteria* (MK603752, 100% sequence identity) (Henson et al., 2020). The highest positive correlation coefficient was observed for the *Terrimonas aquatica* ($\rho = 0.71$) and the *acIV* subcluster A OTUs ($\rho = 0.55$) (Figure 6B). Additionally, 3 OTUs with altogether $>10\%$ of total reads were negatively correlated with total DFAA concentrations: *Polynucleobacter acidiphobus* (CP023277, 100% sequence identity), *Limnohabitans* sp. JirIII-27 (LT717404, 100% sequence identity), and *Polaromonas* (FJ612149, 99.7% sequence identity).

DISCUSSION

Seasonal differences of composition and community assembly processes in FL

Seasonality represents one of the most prominent drivers of change in pelagic microbial assemblages of

lakes, and seasonal differences in FL composition, as observed in our study (Figure 3A, B), are well documented (Allgaier & Grossart, 2006; Eiler et al., 2012; Kara et al., 2013; Kent et al., 2007; Neuenschwander et al., 2018). However, only a few studies have addressed potential seasonal differences in the assembly processes of FL (Jiao et al., 2021), likely because of the high number of biological replicates per time point that are necessary for a null model-based analysis of community assembly (Ning et al., 2019). No specific subset of abundant genotypes preferably grew during October (Table 1). Instead, the community during that season was a mix of 'core' OTUs with high read numbers in either the May or the July assemblages, but not in both. Such taxa were, for example, affiliated with Bacteroidota (*Fluviicola*, *Pseudoarcicella*), or with different genera of *acI* Actinobacteria (data not shown). Currently, it is not clear which environmental factors were responsible for the concurrent success of genotypes in the October samples that appeared to be seasonally well-separated before. It is, for example, conceivable that the epilimnetic bloom of the cyanobacterium *P. rubescens* might allow for the re-growth of taxa in October that were prominent during the spring phytoplankton bloom, while the comparatively high water temperatures (Figure S2) might simultaneously favour the persistence of bacteria from the July assemblage.

Spatial heterogeneity of HNA

HNA represent cells with larger genomes or multiple genome copies; they are regarded as a proxy for the more 'active' or 'opportunistically growing' bacteria within FL (Bouvier et al., 2007; Lebaron et al., 2001). In May, HNA had higher spatial variability than LNA, and their in situ variability was also higher than in a well-mixed large water sample (Figure 1B, Figure S3). This is in line with previous reports of HNA 'hotspots' (Dann et al., 2014; Seymour et al., 2004; Seymour

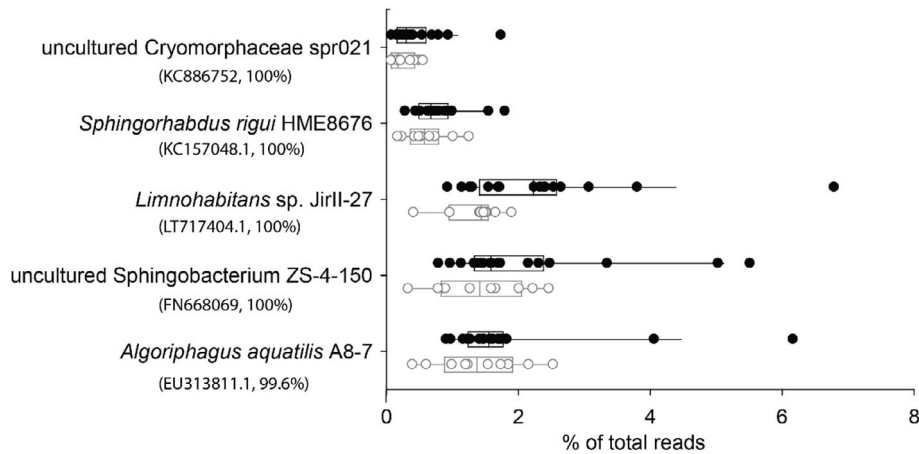


FIGURE 5 Operational taxonomic units (OTUs) with significant spatial variability in syringe samples from May (black symbols and box plots; in brackets: accession number of closest relative and % identity). The read numbers of replicates from the selected OTUs are depicted for reference (grey symbols and box plots). All listed taxa were from free-living (FL).

et al., 2008). Motile bacterial cells are chemotactically attracted to microscale nutrient patches (Blackburn et al., 1998; Raina et al., 2022), and the spatial heterogeneity of HNA might thus be a consequence of the conspicuous phytoplankton bloom in May (Figure S2). In addition, the lack of correlation between HNA and any single OTU suggests that HNA were composed of spatially variable subsets of bacterial genotypes.

Spatial heterogeneity of FL and individual FL taxa

The composition of FL from different syringes in May and July was indistinguishable from technical replicates drawn from a single syringe (Figure 4). This speaks for spatially uniform selection conditions and/or homogenizing dispersion, e.g., mediated by turbulent mixing (Wüest & Lorke, 2003). However, FL from different syringes had significant spatial beta diversity in October, as compared to replicates from single syringes (Figure 4). This was due to higher proportions of rare FL bacteria in the October samples. Rare OTUs in FL were, for example, affiliated with predatory delta-proteobacteria, or with known ‘tychoplanktic’ taxa such as *Sphingomonas*, *Fluviicola*, or *Aeromonas*. Some of these rare OTUs might have originated from small or fragmented particles that passed through the 5 µm pre-filtration, highlighting the limitations of a simple operational division between FL and PA (Malfatti & Azam, 2009; Mestre et al., 2017). Rare ‘tychoplanktic’ bacteria also played a central role in the *de-novo* formation of microbial biofilms from Lake Zurich waters (Silva & Pernthaler, 2020). Our findings indicate that the observed seasonal differences of community assembly processes in such biofilms might be related

to the spatial heterogeneity of ‘tychoplanktic’ taxa and PA bacteria not retained by 5 µm pre-filtration.

Only a few of the large FL OTUs had spatially explicit distribution patterns (Figures 5 and 6). This was likely not related to cell motility: The closest relatives of two spatially variable OTUs from May (Figure 5), *Algoriphagus aquatilis* strain A8-7, and *Spingorhabdus rigui* are non-motile (Baik et al., 2013; Liu et al., 2009), and so are bacteria affiliated with *Terrimonas aquatica* and *Polynucleobacter acidiphobus* (Hahn et al., 2011; Sheu et al., 2010), that were significantly correlated with DFAA concentrations in July (Figure 6). Thus, it is more plausible that local differences in population growth or mortality rates were responsible for the spatial distribution of these OTUs (Dann et al., 2016). Interestingly, several of the spatially variable taxa had elevated read numbers in the same samples (Figure 5). This might either indicate an unidentified artefact, or it might suggest that the same—unknown—factor(s) promoted local growth of more than one FL population.

Spatial heterogeneity of PA

We assume that PA could be readily sampled by our device. For one, smaller particles such as microcolonies could readily pass through the 1 mm openings of the syringes and tubes leading to the sampler. Secondly, the pressure during sampling likely destroyed the larger albeit more fragile ‘lake snow’ aggregates, so that the microbes attached to such structures could also be collected. Evidence for such a disruption and subsequent collection of ‘lake snow’ aggregates is, for example, provided by DFAA concentrations that were elevated by 3 orders of magnitude in some of the syringe samples (Krempaska et al., 2021) (Figure S3).

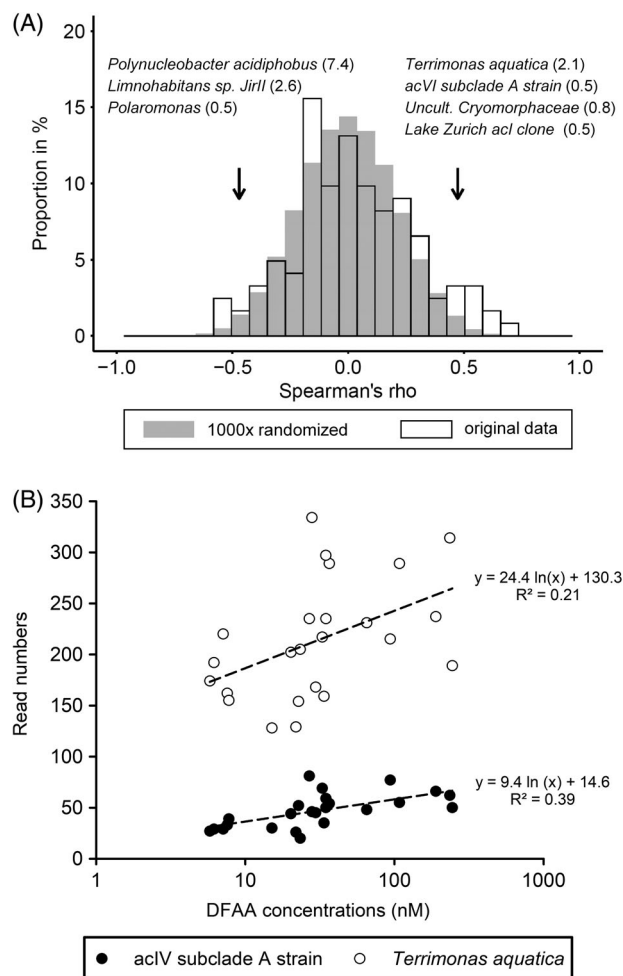


FIGURE 6 (A) Distribution of Spearman correlation coefficients (ρ) of the read numbers of all operational taxonomic units (OTUs) with the concentrations of dissolved free amino acids (DFAA) in 24 syringe samples from July, as compared to 1000 sets of such correlations using randomized DFAA concentrations. Arrows indicate ρ values representing the top and bottom 0.5% of the randomized data set (two-sided $p < 0.01$). Bacterial OTUs with ρ values outside this threshold (all from FL) are listed. Numbers in brackets: proportions of total reads represented by these OTUs. (B) Read numbers of the two OTUs with the highest positive Spearman correlation coefficient vs. DFAA concentrations.

In contrast with previous findings (Mestre et al., 2020; Rösel et al., 2012), seasonality was only weak in PA (Figure 3c). We assume that this was related to our specific sampling scheme, specifically due to the observed high small-scale spatial beta diversity of PA: any single syringe only represented a small fraction of their total seasonal richness, that is, most PA OTUs found in a single sampling campaign were only present in 10% or less of the samples of the respective campaign (Figure 2). In fact, almost half (39%–45%) of PA OTUs were only obtained from one of the 5 technical replicates (i.e., 100 μ L volumes) drawn from a single syringe, indicating a high level of stochasticity at this volume scale. Some of these sporadically occurring

OTUs, for example, genotypes with 100% sequence identity to various Deinococcaceae [KP218915, JF222523, KC634101], or to the bird intestinal tract bacterium *Enterococcus columbae*, had remarkably high read numbers (>1000 reads) within single technical replicate communities, suggesting that they likely originated from taxonomically homogeneous microcolonies.

By contrast, other PA OTUs were distributed across many or even all syringe samples from one or more seasons. For example, one genotype of protein-degrading, particle-attached bacteria of the OM27 clade (Orsi et al., 2016) (FJ612196, 100% sequence identity) was present in every single syringe in May but was absent in July and October. Another OTU, related to a *Pseudomonas* sp. (KM253252, 100% sequence identity), was exclusively found in all syringe samples from October. Most strikingly, an OTU affiliated with the chitin-degrading, nosocomial pathogen *Delftia lacustris* (FJ193562, 100% sequence identity) (Jorgensen et al., 2009; Shin et al., 2012) was present in every single syringe sample from all three seasons but was never found in any of the 5 μ m pre-filtered reference samples.

CONCLUSIONS

We provide first field evidence that PA in lake water exhibited the considerable small-scale spatial heterogeneity predicted by experiments on artificially generated organic aggregates (Bizic-Ionescu et al., 2018) (Figure 2). This may in parts reflect the variable nature of the particulate organic matter in freshwater lakes (algal aggregates, zooplankton excrements or carapaces, etc.), and it speaks for the importance of stochastic community assembly processes (Zhou & Ning, 2017), such as dispersal limitation, during particle colonization. At the same time, the ubiquitous occurrence of some PA OTUs in syringe samples of one or more seasons also highlights the importance of niche-related, deterministic selection during particle colonization, e.g., for polymer-degradation specialists (Enke et al., 2019). Small-scale spatial heterogeneity may also occur in single FL populations (Figure 5) and within the total FL community (Figure 4), for example, due to seasonal maxima of rare, ‘tychoplanktic’ bacteria. Assuming that such small-scale compositional heterogeneity is mirrored by a variable spatial distribution of functional microbial traits, our findings might help to explain the high variability of biological replicates often observed in biotransformation assays of xenobiotic compounds (Seller et al., 2020).

AUTHOR CONTRIBUTIONS

Jakob Pernthaler: Conceptualization (lead); formal analysis (supporting); funding acquisition (lead); project

administration (lead); resources (lead); supervision (lead); writing – original draft (lead); writing – review and editing (lead). **Natalia Krempaska:** Formal analysis (lead); investigation (lead); software (equal); writing – original draft (equal). **Alizée le Moigne:** Formal analysis (supporting); methodology (supporting); writing – review and editing (supporting).


ACKNOWLEDGMENT

Open access funding provided by Universitat Zurich.

DATA AVAILABILITY STATEMENT

The data that support the findings of this study are openly available in figshare at <https://doi.org/10.6084/m9.figshare.c.6637772.v1>.

ORCID

Jakob Pernthaler  <https://orcid.org/0000-0001-7558-909X>

REFERENCES

- Allgaier, M. & Grossart, H.P. (2006) Seasonal dynamics and phylogenetic diversity of free-living and particle-associated bacterial communities in four lakes in northeastern Germany. *Aquatic Microbial Ecology*, 45, 115–128.
- Baik, K.S., Choe, H.N., Park, S.C., Hwang, Y.M., Kim, E.M., Park, C. et al. (2013) *Sphingopyxis rigui* sp nov and *Sphingopyxis woonponensis* sp nov., isolated from wetland freshwater, and emended description of the genus *Sphingopyxis*. *International Journal of Systematic and Evolutionary Microbiology*, 63, 1297–1303.
- Benjamini, Y. & Hochberg, Y. (1995) Controlling the false discovery rate—a practical and powerful approach to multiple testing. *Journal of the Royal Statistical Society Series B-Statistical Methodology*, 57, 289–300.
- Beutler, M., Wiltshire, K.H., Meyer, B., Moldaenke, C., Lüring, C., Meyerhöfer, M. et al. (2002) A fluorometric method for the differentiation of algal populations in vivo and in situ. *Photosynthesis Research*, 72, 39–53.
- Bizic-Ionescu, M., Ionescu, D. & Grossart, H.P. (2018) Organic particles: heterogeneous hubs for microbial interactions in aquatic ecosystems. *Frontiers in Microbiology*, 9. <https://doi.org/10.3389/fmicb.2018.02569>
- Bizic-Ionescu, M., Zeder, M., Ionescu, D., Oric, S., Fuchs, B.M., Grossart, H.P. et al. (2015) Comparison of bacterial communities on limnic versus coastal marine particles reveals profound differences in colonization. *Environmental Microbiology*, 17, 3500–3514.
- Blackburn, N., Fenchel, T. & Mitchell, J. (1998) Microscale nutrient patches in planktonic habitats shown by chemotactic bacteria. *Science*, 282, 2254–2256.
- Bossard, P., Gammeter, S., Lehmann, C., Schanz, F., Bachofen, R., Burgi, H.R. et al. (2001) Limnological description of the lakes Zurich, Lucerne, and Cadagno. *Aquatic Sciences*, 63, 225–249.
- Bouvier, T., del Giorgio, P.A. & Gasol, J.M. (2007) A comparative study of the cytometric characteristics of high and low nucleic acid bacterioplankton cells from different aquatic ecosystems. *Environmental Microbiology*, 9, 2050–2066.
- Chase, J.M., Kraft, N.J.B., Smith, K.G., Vellend, M. & Inouye, B.D. (2011) Using null models to disentangle variation in community dissimilarity from variation in alpha-diversity. *Ecosphere*, 2, 24.
- Chelius, M.K. & Triplett, E.W. (2001) The diversity of archaea and bacteria in association with the roots of *Zea mays* L. *Microbial Ecology*, 41, 252–263.
- Dann, L.M., Mitchell, J.G., Speck, P.G., Newton, K., Jeffries, T. & Paterson, J. (2014) Virio- and Bacterioplankton microscale distributions at the sediment-water interface. *PLoS One*, 9, e102805.
- Dann, L.M., Smith, R.J., Tobe, S.S., Paterson, J.S., Oliver, R.L. & Mitchell, J.G. (2016) Microscale distributions of freshwater planktonic viruses and prokaryotes are patchy and taxonomically distinct. *Aquatic Microbial Ecology*, 77, 65–77.
- Datta, M.S., Sliwerska, E., Gore, J., Polz, M.F. & Cordero, O.X. (2016) Microbial interactions lead to rapid micro-scale successions on model marine particles. *Nature Communications*, 7, 11965.
- Edgar, R.C. (2016) UNOISE2: improved error-correction for Illumina 16S and ITS amplicon sequencing. *bioRxiv*.
- Eiler, A., Heinrich, F. & Bertilsson, S. (2012) Coherent dynamics and association networks among lake bacterioplankton taxa. *ISME Journal*, 6, 330–342.
- Enke, T.N., Datta, M.S., Schwartzman, J., Cermak, N., Schmitz, D., Barrere, J. et al. (2019) Modular assembly of polysaccharide-degrading marine microbial communities. *Current Biology*, 29, 1528.
- Grossart, H.P. & Simon, M. (1998) Bacterial colonization and microbial decomposition of limnetic organic aggregates (lake snow). *Aquatic Microbial Ecology*, 15, 127–140.
- Hahn, M.W., Lang, E., Brandt, U. & Sproer, C. (2011) *Polynucleobacter acidiphobus* sp. nov., a representative of an abundant group of planktonic freshwater bacteria. *International Journal of Systematic and Evolutionary Microbiology*, 61, 788–794.
- Henson, M.W., Lanclos, V.C., Pitre, D.M., Weckhorst, J.L., Lucchesi, A.M., Cheng, C. et al. (2020) Expanding the diversity of Bacterioplankton isolates and modeling isolation efficacy with large-scale dilution-to-extinction cultivation. *Applied and Environmental Microbiology*, 86, e00943–e00920.
- Hervé, M. (2020) *RVAideMemoire: testing and plotting procedures for biostatistics*. R package version 0.9-73. The R Foundation. <https://CRAN.R-project.org/package=RVAideMemoire>
- Horňák, K., Schmidheiny, H. & Pernthaler, J. (2016) High-throughput determination of dissolved free amino acids in unconcentrated freshwater by ion-pairing liquid chromatography and mass spectrometry. *Journal of Chromatography A*, 1440, 85–93.
- Hu, Y., Xie, G.J., Jiang, X.Y., Shao, K.Q., Tang, X.M. & Gao, G. (2020) The relationships between the free-living and particle-attached bacterial communities in response to elevated eutrophication. *Frontiers in Microbiology*, 11. <https://doi.org/10.3389/fmicb.2020.00423>
- Imboden, D.M. & Wuest, A. (1995) Mixing mechanisms in lakes. In: A. Lerman, D. M. Imboden, & J. R. Gat (Eds.), *Physics and Chemistry of Lakes*. Springer. https://doi.org/10.1007/978-3-642-85132-2_4
- Jiao, C.C., Zhao, D.Y., Huang, R., He, F. & Yu, Z.B. (2021) Habitats and seasons differentiate the assembly of bacterial communities along a trophic gradient of freshwater lakes. *Freshwater Biology*, 66, 1515–1529.
- Jones, S.E., Cadkin, T.A., Newton, R.J. & McMahon, K.D. (2012) Spatial and temporal scales of aquatic bacterial beta diversity. *Frontiers in Microbiology*, 3. <https://doi.org/10.3389/fmicb.2012.00318>
- Jorgensen, N.O.G., Brandt, K.K., Nybroe, O. & Hansen, M. (2009) *Delftia lacustris* sp nov., a peptidoglycan-degrading bacterium from fresh water, and emended description of *Delftia tsuruhatensis* as a peptidoglycan-degrading bacterium. *International Journal of Systematic and Evolutionary Microbiology*, 59, 2195–2199.
- Kara, E.L., Hanson, P.C., Hu, Y.H., Winslow, L. & McMahon, K.D. (2013) A decade of seasonal dynamics and co-occurrences within freshwater bacterioplankton communities from eutrophic Lake Mendota, WI, USA. *ISME Journal*, 7, 680–684.

- Kent, A.D., Yannarell, A.C., Rusak, J.A., Triplett, E.W. & McMahon, K.D. (2007) Synchrony in aquatic microbial community dynamics. *ISME Journal*, 1, 38–47.
- Kjørboe, T. & Jackson, G.A. (2001) Marine snow, organic solute plumes, and optimal chemosensory behavior of bacteria. *Limnology and Oceanography*, 46, 1309–1318.
- Krempaska, N., Hornak, K., Silva, M.O.D. & Pernthaler, J. (2021) Spatial microheterogeneity and selective microbial consumption of dissolved free amino acids in an oligomesotrophic lake. *Limnology Oceanography*, 66, 3728–3739.
- Lampitt, R.S., Hillier, W.R. & Challenor, P.G. (1993) Seasonal and diel variation in the Open Ocean concentration of marine snow aggregates. *Nature*, 362, 737–739.
- Lear, G., Bellamy, J., Case, B.S., Lee, J.E. & Buckley, H.L. (2014) Fine-scale spatial patterns in bacterial community composition and function within freshwater ponds. *The ISME Journal*, 8, 1715–1726.
- Lebaron, P., Servais, P., Agogue, H., Courties, C. & Joux, F. (2001) Does the high nucleic acid content of individual bacterial cells allow us to discriminate between active cells and inactive cells in aquatic systems? *Applied and Environmental Microbiology*, 67, 1775–1782.
- Liu, Y., Li, H., Jiang, J.T., Liu, Y.H., Song, X.F., Xu, C.J. et al. (2009) *Algoriphagus aquatilis* sp. nov., isolated from a freshwater lake. *International Journal of Systematic and Evolutionary Microbiology*, 59, 1759–1763.
- Malfatti, F. & Azam, F. (2009) Atomic force microscopy reveals microscale networks and possible symbioses among pelagic marine bacteria. *Aquatic Microbial Ecology*, 58, 1–14.
- Mestre, M., Borrell, E., Sala, M.M. & Gasol, J.M. (2017) Patterns of bacterial diversity in the marine planktonic particulate matter continuum. *ISME Journal*, 11, 999–1010.
- Mestre, M., Hofer, J., Sala, M.M. & Gasol, J.M. (2020) Seasonal variation of bacterial diversity along the marine particulate matter continuum. *Frontiers in Microbiology*, 11. <https://doi.org/10.3389/fmicb.2020.01590>
- Möller, K.O., St John, M., Temming, A., Floeter, J., Sell, A.F., Herrmann, J.P. et al. (2012) Marine snow, zooplankton and thin layers: indications of a trophic link from small-scale sampling with the video plankton recorder. *Marine Ecology Progress Series*, 468, 57–69.
- Morlon, H., Chuyong, G., Condit, R., Hubbell, S., Kenfack, D., Thomas, D. et al. (2008) A general framework for the distance-decay of similarity in ecological communities. *Ecology Letters*, 11, 904–917.
- Neuenschwander, S.M., Ghai, R., Pernthaler, J. & Salcher, M.M. (2018) Microdiversification in genome-streamlined ubiquitous freshwater Actinobacteria. *ISME Journal*, 12, 185–198.
- Ning, D., Deng, Y., Tiedje, J.M. & Zhou, J. (2019) A general framework for quantitatively assessing ecological stochasticity. *Proceedings of the National Academy of Sciences*, 116, 16892–16898.
- Okazaki, Y., Fujinaga, S., Tanaka, A., Kohzu, A., Oyagi, H. & Nakano, S. (2017) Ubiquity and quantitative significance of bacterioplankton lineages inhabiting the oxygenated hypolimnion of deep freshwater lakes. *ISME Journal*, 11, 2279–2293.
- Oksanen, J., Blanchet, F., Friendly, M., Kindt, R., Legendre, P., McGinn, D. et al. (2018) *Vegan: community ecology package. R package version 2.5–2. 2018*. Vienna: R Core Team.
- Orsi, W.D., Smith, J.M., Liu, S.T., Liu, Z.F., Sakamoto, C.M., Wilken, S. et al. (2016) Diverse, uncultivated bacteria and archaea underlying the cycling of dissolved protein in the ocean. *ISME Journal*, 10, 2158–2173.
- Paradis, E. & Schliep, K. (2019) Ape 5.0: an environment for modern phylogenetics and evolutionary analyses in R. *Bioinformatics*, 35, 526–528.
- Posch, T., Köster, O., Salcher, M.M. & Pernthaler, J. (2012) Harmful filamentous cyanobacteria favoured by reduced water turnover with lake warming. *Nature Climate Change*, 2, 809–813.
- Quast, C., Pruesse, E., Yilmaz, P., Gerken, J., Schweer, T., Yarza, P. et al. (2013) The SILVA ribosomal RNA gene database project: improved data processing and web-based tools. *Nucleic Acids Research*, 41, D590–D596.
- Raina, J.B., Lambert, B.S., Parks, D.H., Rinke, C., Siboni, N., Bramucci, A. et al. (2022) Chemotaxis shapes the microscale organization of the ocean's microbiome. *Nature*, 605, 132–138.
- Rösel, S., Allgaier, M. & Grossart, H.P. (2012) Long-term characterization of free-living and particle-associated bacterial communities in Lake Tiefwaren reveals distinct seasonal patterns. *Microbial Ecology*, 64, 571–583.
- Salcher, M.M., Hofer, J., Horňák, K., Jezbera, J., Sonntag, B., Vrba, J. et al. (2007) Modulation of microbial predator–prey dynamics by phosphorus availability: growth patterns and survival strategies of bacterial phylogenetic clades. *FEMS Microbiology Ecology*, 60, 40–50.
- Salcher, M.M., Pernthaler, J., Frater, N. & Posch, T. (2011) Vertical and longitudinal distribution patterns of different bacterioplankton populations in a canyon-shaped, deep prealpine lake. *Limnology and Oceanography*, 56, 2027–2039.
- Seller, C., Honti, M., Singer, H. & Fenner, K. (2020) Biotransformation of chemicals in water-sediment suspensions: influencing factors and implications for persistence assessment. *Environmental Science & Technology Letters*, 7, 854–860.
- Seymour, J.R., Amin, S.A., Raina, J.B. & Stocker, R. (2017) Zooming in on the phycosphere: the ecological interface for phytoplankton–bacteria relationships. *Nature Microbiology*, 2, 17065.
- Seymour, J.R., Mitchell, J.G. & Seuront, L. (2004) Microscale heterogeneity in the activity of coastal bacterioplankton communities. *Aquatic Microbial Ecology*, 35, 1–16.
- Seymour, J.R., Seuront, L., Doubell, M.J. & Mitchell, J.G. (2008) Mesoscale and microscale spatial variability of bacteria and viruses during a *Phaeocystis globosa* bloom in the Eastern English Channel. *Estuarine Coastal and Shelf Science*, 80, 589–597.
- Seymour, J.R., Seuront, L., Doubell, M., Waters, R.L. & Mitchell, J.G. (2006) Microscale patchiness of virioplankton. *Journal of the Marine Biological Association of the United Kingdom*, 86, 551–561.
- Sheu, S.Y., Cho, N.T., Arun, A.B. & Chen, W.M. (2010) *Terrimonas aquatica* sp. nov., isolated from a freshwater spring. *International Journal of Systematic and Evolutionary Microbiology*, 60, 2705–2709.
- Shin, S.Y., Choi, J.Y. & Ko, K.S. (2012) Four cases of possible human infections with *Delftia lacustris*. *Infection*, 40, 709–712.
- Silva, M.O.D., Blom, J.F., Yankova, Y., Villiger, J. & Pernthaler, J. (2018) Priming of microbial microcystin degradation in biomass-fed gravity driven membrane filtration biofilms. *Systematic and Applied Microbiology*, 41, 221–231.
- Silva, M.O.D. & Pernthaler, J. (2020) Biomass addition alters community assembly in ultrafiltration membrane biofilms. *Scientific Reports*, 10, 11552. <https://doi.org/10.1038/s41598-020-68460-x>
- Soininen, J., McDonald, R. & Hillebrand, H. (2007) The distance decay of similarity in ecological communities. *Ecography*, 30, 3–12.
- Tang, X.M., Gao, G., Chao, J.Y., Wang, X.D., Zhu, G.W. & Qin, B.Q. (2010) Dynamics of organic-aggregate-associated bacterial communities and related environmental factors in Lake Taihu, a large eutrophic shallow lake in China. *Limnology and Oceanography*, 55, 469–480.
- Vincent, A. & Meneguzzi, M. (1991) The spatial structure and statistical properties of homogeneous turbulence. *Journal of Fluid Mechanics*, 225, 1–20.

- Wüest, A. & Lorke, A. (2003) Small-scale hydrodynamics in lakes. *Annual Review of Fluid Mechanics*, 35, 373–412.
- Zhou, J. & Ning, D. (2017) Stochastic community assembly: does it matter in microbial ecology? *Microbiology and Molecular Biology Reviews*, 81(4), e00002-17

SUPPORTING INFORMATION

Additional supporting information can be found online in the Supporting Information section at the end of this article.

How to cite this article: Pernthaler, J., Krempaska, N. & le Moigne, A. (2023) Small-scale spatial beta diversity of bacteria in the mixed upper layer of a lake. *Environmental Microbiology*, 1–13. Available from: <https://doi.org/10.1111/1462-2920.16399>